

## InP/InGaAs Heterojunction Bipolar Transistor with Base $\mu$ -Bridge and Emitter Air-Bridge<sup>\*</sup>

Yu Jinyong<sup>1</sup>, Liu Xinyu<sup>1,†</sup>, Su Shubing<sup>1</sup>, Wang Runmei<sup>1</sup>, Xu Anhuai<sup>2</sup>, and Qi Ming<sup>2</sup>

(1 Institute of Microelectronics, Chinese Academy of Sciences, Beijing 100029, China)

(2 Shanghai Institute of Microsystem and Information Technology, Chinese Academy of Sciences, Shanghai 200050, China)

**Abstract:** An InP-based single-heterojunction bipolar transistor (SHBT) with base  $\mu$ -bridge and emitter air-bridge is reported. Because those bridges reduce parasitic capacitance greatly, the cutoff frequency  $f_T$  of the  $2\mu\text{m} \times 12.5\mu\text{m}$  InP SHBT without de-embedding reaches 178GHz. It is critical in high-speed low power applications, such as OEIC receivers and analog-to-digital converters.

**Key words:** InP; HBT;  $\mu$ -bridge; air-bridge; self-aligning

**EEACC:** 2560J

**CLC number:** TN385

**Document code:** A

**Article ID:** 0253-4177(2007)02-0154-05

### 1 Introduction

InP/InGaAs SHBTs have many advantages for high-speed and low power applications owing to the excellent properties of InP and InGaAs<sup>[1]</sup>, although they suffer from low breakdown voltage<sup>[2]</sup>. In order to improve the performance of InP/InGaAs SHBTs, many technologies have been developed to minimize its parasitics<sup>[3,4]</sup>. Most of these technologies deal with the parasitic base-collector capacitor (B-C capacitor), base-emitter capacitor (B-E capacitor), and base resistance. The presence of extrinsic base and emitter pads contributes to a fairly large portion of the B-C capacitance and B-E capacitance. However, the reduction of the extrinsic base or emitter pad area by narrowing their width directly introduces higher resistance and reactance<sup>[5]</sup>. Some research on InP/InGaAs HBT has been done previously. For example, a self-aligned InP/InGaAs SHBT using a T-shaped emitter was reported by Su *et al.*<sup>[6]</sup>. In his work, the current gain cutoff frequency and the maximum oscillation frequency of the device were 85 and 72GHz, respectively. The  $f_T$  of a self-aligned InP/InGaAs SHBT with a  $1\mu\text{m}$  emitter reported recently was 162GHz, and the  $f_{\text{max}}$  was 50GHz<sup>[7]</sup>. In addition, an InP/GaAs<sub>0.5</sub>Sb<sub>0.5</sub>/InP

DHBT with  $f_T$  higher than 100GHz was reported by Xu and Watkins<sup>[8]</sup>. However, they do not give an effective method to reduce parasitic capacitance and inductance.

An HBT with base  $\mu$ -bridge and emitter air-bridge is reported in this paper. Self-aligned emitter technology is utilized to reduce parasitic base resistance. Due to the effect of bridges and self-aligning, the cutoff frequency  $f_T$  of the  $2\mu\text{m} \times 12.5\mu\text{m}$  InP/InGaAs HBT without de-embedding reaches 178GHz at a collector current of  $I_C = 33.7\text{mA}$ . The maximum oscillation frequency  $f_{\text{max}}$  is 60GHz, the maximum DC gain is 87.5, and the offset voltage is 0.10V.

### 2 Design and fabrication

It is well known that the selective wet etching of InP by HCl: H<sub>3</sub>PO<sub>4</sub> has strong anisotropic effects<sup>[9]</sup>. The etching rate is higher in crystal directions parallel to [001] and [010]. The lack of undercut under the emitter edge parallel to the [01 $\bar{1}$ ] direction makes self-aligned structures impossible without massive over etching<sup>[9]</sup>. The etching rate in directions parallel to [001] and [010] is so high that it is fatal to narrow emitter HBTs. For forming  $\mu$ -bridges and self-aligning, [011],

<sup>\*</sup> Project supported by the State Key Development Program for Basic Research of China (No.2002CB311903) and the Innovation Program of the Chinese Academy of Sciences (No.KGCX2-107)

<sup>†</sup> Corresponding author. Email: xyliu@ime.ac.cn

Received 11 August 2006, revised manuscript received 12 September 2006

©2007 Chinese Institute of Electronics

$[001]$ , and  $[010]$  are all available directions. However, only in the direction parallel to  $[011]$  is the etching rate appropriate to form a self-aligned emitter. In order to avoid a short circuit in the direction parallel to  $[01\bar{1}]$  between the base and emitter, it is wise to use a hexagonal emitter metal design<sup>[10]</sup>.

The base pad of one kind of conventional InP HBT is shown in Fig. 1(a). The base and collector regions overlap under the base metal outside the intrinsic HBT. This apparently increases parasitic B-C capacitance. The emitter pad has the same

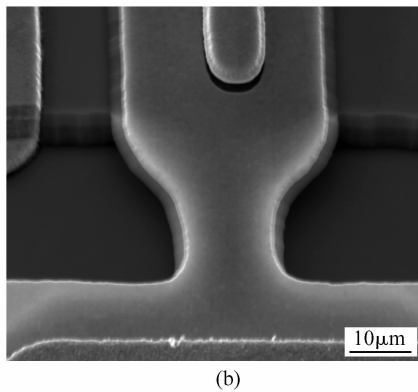
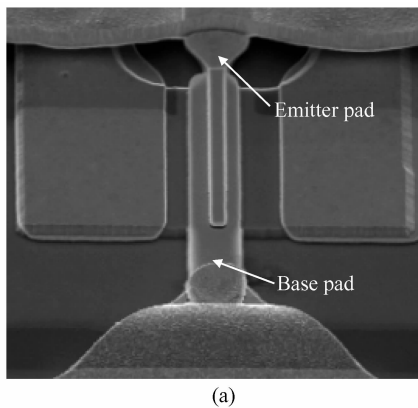


Fig. 1 (a) Base and emitter pads of conventional InP HBT; (b) SEM picture of a base  $\mu$ -bridge between base pad and intrinsic HBT formed by lateral etching of InGaAs and InP

problem, which increases the parasitic B-C and B-E capacitances. Thus the performance of the HBT will increase greatly if these parasitics are minimized. The use of base  $\mu$ -bridge and emitter air-bridge is an effective way to solve the problem. If the base electrodes are connected to the pads through a metal bridge under which there is no epitaxial layer, as shown in Fig. 1(b), then the

parasitic capacitance under the pads is open-circuit and will almost never affect the performance of the HBT. The formation of a base  $\mu$ -bridge also makes use of the strong anisotropic effects of InP just mentioned before. Owing to the lateral etching in the direction parallel to  $[011]$ , the InP and InGaAs materials under the base metal between the intrinsic base and base pad can be removed with long enough etching time. The emitter air-bridge connects the emitter to the pad by forming a wide metal over the collector in the air. It reduces parasitic capacitance and emitter inductance.

In this work, base  $\mu$ -bridge, emitter air-bridge, and self-aligning technologies are used. The emitter is designed to be hexagonal. In order to minimize the B-C capacitance, the width of the base metal is designed to be only  $1\mu\text{m}$ . The fabrication process is as follows.

The epitaxial layers are grown on Fe-doped semi-insulating (100) InP substrate by MOCVD. Silicon is used for n-type dopant, and beryllium (Be) for p-type dopant. The emitter contact layer and sub-collector layer are both InGaAs. A 120nm thick InP layer is grown as the emitter. The base is InGaAs with a thickness of 50nm and p-type carrier concentration of  $3 \times 10^{19} \text{ cm}^{-3}$ . A 5nm undoped InGaAs layer between the emitter and the base is for stopping the diffusion of Be impurity from the base to the emitter. InGaAs is used for both the base and the collector, which enhances the speed of the SHBT.

The devices are fabricated using a standard mesa process with wet chemical etching and contact photolithography. The fabrication process starts with the formation of the  $2\mu\text{m} \times 12.5\mu\text{m}$  emitter electrodes on the top of the InGaAs layer by photolithography and the lift-off technique. Selective wet etching is used to form an appropriate undercut around the emitter mesa and to reveal the base layer. The base metal of Ti/Pt/Au is then evaporated over the base region, including the entire emitter metal. Base and collector layers are etched, and then the sub-collector layer is etched until the semi-insulating InP substrate is revealed. During all these etching processes, the base area between the base pad and the intrinsic HBT is uncovered by photoresist, and lateral etching is used. Because the etching time is long e-

nough, the InP and InGaAs are removed from under the bridge metal which forms the  $\mu$ -bridge. After Ti/Pt/Au for the collector ohmic contact is evaporated and lifted-off, a very thick photoresist block is formed over the collector metal. An interconnection metal is then evaporated to connect the electrodes of the transistors to the pads. After the photoresist is removed, the emitter air-bridge is formed. A scanning electron micrograph (SEM) image of the device is shown in Fig. 2.

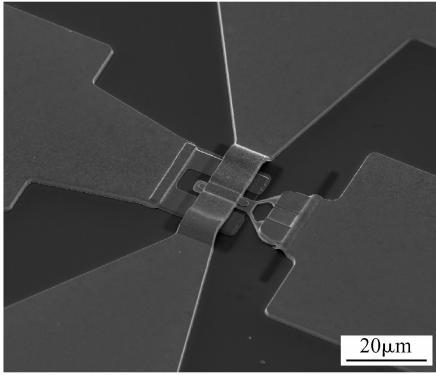


Fig. 2 SEM image of the  $2\mu\text{m} \times 12.5\mu\text{m}$  InP SHBT

### 3 Results and discussion

The common emitter output characteristics are shown in Fig. 3, where the offset voltage is approximately 0.1 V, the knee voltage is 0.3 V at  $I_C = 7\text{mA}$ , the common emitter breakdown voltage is 3.8 V, and the current gain is about 87.5 at  $I_C = 7\text{mA}$ .

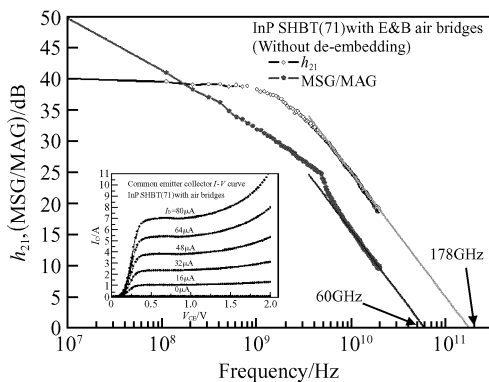


Fig. 3 Collector  $I$ - $V$  and RF characteristics of the  $2\mu\text{m} \times 12.5\mu\text{m}$  InP SHBT

RF performances of the InP/InGaAs HBTs are characterized with an HP8510C network analyzer. The current gain and the maximum stable/available gain (MSG/MAG) for the  $2\mu\text{m} \times$

$12.5\mu\text{m}$  HBT are also shown in Fig. 3. The extrapolated  $f_T$  is 178 GHz and  $f_{\text{max}}$  is 60 GHz.  $f_T$  and  $f_{\text{max}}$  reach their maximum values at  $I_C = 33.7\text{mA}$ . The measurement is taken without de-embedding.

Figure 4 shows a comparison of the RF performance of three kinds of InP HBTs on the same wafer. All the three kinds of HBT are fabricated with self-aligned technology. However, the InP HBT with base  $\mu$ -bridge and emitter air-bridge shows the highest cutoff frequency. The  $f_T$  and  $f_{\text{max}}$  of the  $2\mu\text{m}$  emitter InP HBT with the air-bridges, conventional  $1\mu\text{m}$  emitter InP HBT, and conventional  $2\mu\text{m}$  emitter InP HBT are 178 GHz/60 GHz, 162 GHz/53 GHz, and 142 GHz/42 GHz, respectively. Therefore the bridges noticeably reduce the parasitics.

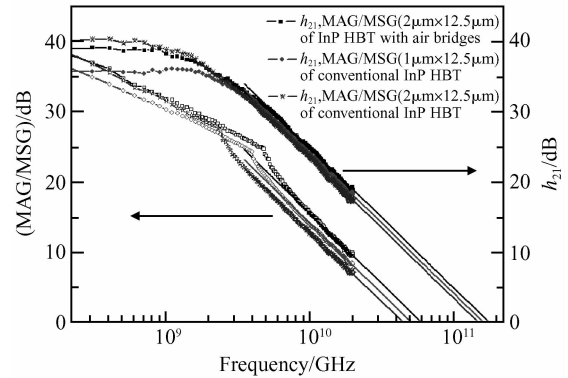


Fig. 4 Comparison of current gain, maximum stable/available gain of InP HBTs on the same wafer among HBT with air-bridges and two conventional InP HBTs with different emitter widths

According to Eq. (1),  $f_T$  shows an increasing trend when  $C_{BC}$  and  $C_{je}$  are reduced. In this work, the base  $\mu$ -bridge reduces the base collector capacitance  $C_{BC}$  and the emitter air-bridge reduces  $C_{BC}$  and  $C_{je}$  so that a high  $f_T$  is achieved.

$$f_T = \frac{1}{2\pi} \times \left[ \frac{\eta k T}{q I_C} (C_{je} + C_{BC}) + \frac{X_B^2}{\nu D_n} + \frac{X_{dep}}{2\nu_{sat}} + (R_E + R_C) C_{BC} \right]^{-1} \quad [1] \quad (1)$$

As shown in Fig. 4, the  $f_{\text{max}}$  of all three kinds of HBT are about 100 GHz lower than  $f_T$ .  $f_{\text{max}}$  is described by the equation  $f_{\text{max}} = \sqrt{f_T / 8\pi r_B C_{BC}}$  [1]. Although  $C_{BC}$  is reduced by using a base  $\mu$ -bridge and emitter air-bridge, the undoped InGaAs layer between base and emitter increases the base sheet resistance greatly, leading to high parasitic base resistance. Thus  $f_{\text{max}}$  is decreased [7]. However, this is not the main reason.

The  $S_{12}$  value of the open testing pads is measured, which represents the coupling of the signal between the input pad and the output pad. The coupling effect cannot be eliminated if the measurement is taken without de-embedding. As shown in Fig. 5, at low frequencies, the  $S_{12}$  of the open testing pads is very small compared to the  $S_{12}$  of the InP HBT. However, at high frequencies, the  $S_{12}$  of the open testing pads is comparable to that of InP HBT. According to the equation

$$\text{MSG} = \left| \frac{S_{21}}{S_{12}} \right|$$

$$\text{MAG} = \left| \frac{S_{21}}{S_{12}} \right| (K - \sqrt{K^2 - 1})$$

where

$$K = \frac{1 - |S_{11}|^2 - |S_{22}|^2 + |\Delta|^2}{2|S_{12}S_{21}|}$$

$f_{\max}$  is proportional to  $1/|S_{12}|$ . At high frequencies, the signal coupling gets stronger, and that leads to high  $|S_{12}|$  and low  $f_{\max}$ .

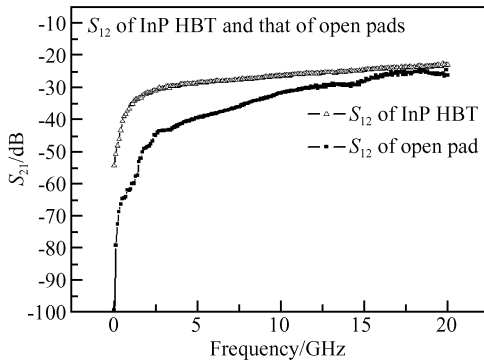


Fig.5  $S_{12}$  of the InP HBT and the open testing pads

## 4 Conclusions

An InP HBT with high cutoff frequency is fabricated by a conventional wet chemical etching process. Because base  $\mu$ -bridge, emitter air-bridge, and self-aligned technologies are used, which min-

imize parasitics, the cutoff frequency of the  $2\mu\text{m} \times 12.5\mu\text{m}$  InP/InGaAs SHBT is as high as 178 GHz. However, the measurement is taken without de-embedding and the signal coupling between testing pads cannot be eliminated, so the extrapolated  $f_{\max}$  is only 60GHz.

**Acknowledgement** The authors would like to thank all the members of the Microwave Devices and Integrated Circuits Department of IMECAS.

## References

- [1] Liu W. Handbook of III-V heterojunction bipolar transistors. Wiley-Interscience Publisher, 1998
- [2] Dvorak M W, Matine N, Bolognesia C R. Design and performance of InP/GaAsSb/InP double heterojunction bipolar transistors. J Vac Sci Technol A, 2000, 18(2): 761
- [3] Hafez W, Lai J W, Feng M. InP/InGaAs SHBTs with 75nm collector and  $f_T > 500\text{GHz}$ . Electron Lett, 2003, 39(20): 1475
- [4] Hayama N, Madihianm M, Okamoto A, et al. Self-aligned AlGaAs/GaAs heterojunction bipolar transistors for high speed integrated-circuits application. IEEE Trans Electron Devices, 1988, 35(11): 1771
- [5] Miyamoto Y, Rios J M M, Dentai A G, et al. Reduction of base-collector capacitance by undercutting the collector and subcollector in GaInAs/InP DHBT's. IEEE Electron Device Lett, 1996, 17(3): 97
- [6] Su Shubing, Liu Xunchun, Liu Xinyu, et al. Performance of a self-aligned InP/GaInAs SHBT with a novel T-shaped emitter. Chinese Journal of Semiconductors, 2006, 27(3): 434
- [7] Yu Jinyong, Yan Beiping, Su Shubing, et al. A 162GHz self-aligned InP/InGaAs heterojunction bipolar transistor. Chinese Journal of Semiconductors, 2006, 27(10): 1732
- [8] Xu X G, Watkins S P. GaAsSb/InP heterojunction bipolar transistors. Research & Progress of SSE, 2001, 21(1): 117 (in Chinese) [徐现刚, Watkins S P. GaAsSb/InP 异质结三极管. 固体电子学研究进展, 2001, 21(1): 117]
- [9] Elias P, Kostic I, Hasenohrl S. Polar diagram of wet-etched [100] InP. International Conference on Indium Phosphide and Related Materials, 2002: 229
- [10] Matine N, Dvorak M W, Pelouard J L, et al. InP in HBTs by vertical and lateral wet etching. International Conference on Indium Phosphide and Related Materials, 1998: 195

## 基极微空气桥和发射极空气桥的 InP/InGaAs HBT<sup>\*</sup>

于进勇<sup>1</sup> 刘新宇<sup>1,†</sup> 苏树兵<sup>1</sup> 王润梅<sup>1</sup> 徐安怀<sup>2</sup> 齐 鸣<sup>2</sup>

(1 中国科学院微电子研究所, 北京 100029)

(2 中国科学院上海微系统与信息技术研究所, 上海 200050)

**摘要:** 报道了具有基极微空气桥和发射极空气桥结构的 InP 单异质结双极型晶体管(SHBT). 由于基极微空气桥和发射极空气桥结构有效地减小了寄生, 发射极尺寸为  $2\mu\text{m} \times 12.5\mu\text{m}$  的 InP HBT 的截止频率达到了 178GHz. 这种器件对高速低功耗的应用非常关键, 例如 OEIC 接收机以及模拟、数字转换器.

**关键词:** InP; 异质结双极型晶体管; 微空气桥; 空气桥; 自对准

EEACC: 2560J

中图分类号: TN385

文献标识码: A

文章编号: 0253-4177(2007)02-0154-05

<sup>\*</sup> 国家重点基础研究发展规划(批准号:2002CB311903)及中国科学院创新基金(批准号:KGCX2-107)资助项目

<sup>†</sup> 通信作者, Email: xylu@ime.ac.cn

2006-08-11 收到, 2006-09-12 定稿